Theoretical resonant Raman spectra of nanotube (7,0) with point defects

ARTICLE *in* PHYSICA STATUS SOLIDI (B) · DECEMBER 2009

Impact Factor: 1.49 · DOI: 10.1002/pssb.200982279

2 AUTHORS:

Valentin N. Popov
Sofia University "St. Kliment Ohridski"
114 PUBLICATIONS **3,844** CITATIONS
SEE PROFILE

Philippe Lambin
University of Namur
295 PUBLICATIONS **7,911** CITATIONS
SEE PROFILE

Theoretical resonant Raman spectra of nanotube (7,0) with point defects

Valentin N. Popov[*,1] and Philippe Lambin[2]

[1] Faculty of Physics, University of Sofia, 5 J. Bourchier Blvd, BG-1164 Sofia, Bulgaria
[2] Research Center in Physics of Matter and Radiation, Facultés Universitaires Notre-Dame de la Paix, 61 rue de Bruxelles, B-5000 Namur, Belgium

Received ZZZ, revised ZZZ, accepted ZZZ
Published online ZZZ (Dates will be provided by the publisher.)

PACS 61.48.De, 63.22.Gh, 73.22.-f, 78.30.Na, 78.67.Ch

* Corresponding author: e-mail vpopov@phys.uni-sofia.bg, Phone: +359 2 8161833, Fax: +359 2 9625276

The Raman spectra of the nanotube (7,0) with point defects (monovacancy, divacancy, and Stone-Wales defect) were simulated in order to derive spectroscopic signatures of defective nanotubes. First, we calculated the electronic band structure and the phonon dispersion of the defective nanotubes using supercells within a non-orthogonal tight-binding model. We found that new optical transitions and Raman-active phonons appeared in comparison with the perfect nanotube. Secondly, we calculated the resonance Raman excitation profile for all Raman-active phonons of the defective nanotubes and simulated their Raman spectra at specific laser excitation energies. The predicted high-intensity Raman lines can be used as spectroscopic signatures of the defective nanotubes.

1 Introduction Carbon nanotubes have been extensively studied both experimentally and theoretically [1]. While a relatively simple description of the nanotube properties can be achieved by using the perfect nanotube structure, in many cases it is crucial to take into account the presence of defects. The mechanical behaviour of nanotubes upon strain is determined by spontaneous formation of Stone-Wales (SW) defects [2]. Defects, even in small density, can change dramatically the electronic transport in nanotubes [3]. Recently, a study of the role of defects in single-walled carbon nanotube sensors has been reported [4]. The electron-defect scattering processes can produce strong bands in the Raman spectra [5]. Therefore, it is of principal importance to have a reliable tool for quantitative characterization of the type and the density of the defects. The Raman scattering spectroscopy has proven to be a powerful and straightforward experimental method for characterization of nanotube samples [1]. This method requires explicit knowledge of the spectroscopic signatures of the various types of defects.

The theoretical prediction of the characteristic phonons of nanotube (3,3) with a SW defect has been obtained by means of the density functional theory [6]. The vibrational modes of nanotube intramolecular junctions have been calculated using the Brenner reactive empirical bond order potential [7]. Recently, the phonon frequencies of zigzag nanotubes with a single monovacancy (MV) defect have been derived using the frozen phonon approach within the density functional theory [8] and a tight-binding model [9]. To our knowledge, phonons in nanotubes with more complex defects like divacancy (DV), etc., have not been reported so far. The latter three studies of phonons are limited to the estimation of the non-resonant Raman intensity of the defect-associated phonons. However, Raman scattering in carbon nanotubes is essentially resonant [1] and any calculations of the non-resonant intensity may be of limited application.

Here, we calculate the resonant Raman spectra of nanotube (7,0) with a MV, DV, and SW defect within a density-functional-theory-based non-orthogonal tight-binding (NOTB) model and discuss the most intense Raman lines as spectroscopic signatures for nanotubes with specific defects.

2 Theoretical background In this study, we focus on nanotube (7,0) with a single MV, DV, or SW defect. One possible model structure would be a nanotube of finite length with free dangling bonds at the ends or with H-

terminated ends. Another possibility would be to consider a supercell with a single defect, which is repeated periodically along the supercell axis to form a nanotube. We chose the latter approach and adopted a supercell, consisting of two nanotube unit cells with a translation period of 8.51 Å. For such supercell the effect of defect-defect interactions is relatively small. The calculation of the band structure and the total energy was performed within the NOTB model [10]. The nanotube structure was relaxed using 10 **k**-points in one half of the Brillouin zone of the nanotube until residual forces on atoms decreased below 0.01 eV/Å. The dynamical matrix was derived using a perturbative approach within the NOTB model [11]. The calculation of the phonons was done with 2 **k**-points. The resonance Raman excitation profiles (REP) of all Raman-active phonons was obtained by means of a quantum-mechanical expression for one-phonon Stokes scattering processes [12]. The convergence of the sum over the Brillouin zone in this expression was reached with as many as 100 **k**-points. The calculation of the intensity was restricted to parallel scattering geometry and the intensity was averaged over nanotube orientation.

Finally, we note that the NOTB model underestimates the measured optical transition energies of small- and moderate-diameter nanotubes by about 0.3 eV [10] and overestimates the observed phonon frequencies by about 11% [11]. For better agreement with experimental data, everywhere below the NOTB transition energies were uphifted and the phonon frequencies were downscaled correspondingly.

3 Results and discussion In a perfect nanotube, all atoms lie on a cylindrical surface but the introduction of defects results in relaxation of the atoms to equilibrium positions generally off this surface. Apart from that, the bond lengths and bond angles change in the vicinity of the defect.

The relaxed nanotubes with a single MV, DV, or SW defect are shown in Figs. 1 and 2. In the structure with a MV defect, the three atoms with dangling bonds, remaining after removing an atom, form a covalent bond of length 1.55 Å. The two atoms at the end of this bond are displaced radially inwards by 0.28 Å, while the third atom is displaced radially outwards by 0.31 Å relative to the average nanotube radius. In the structure with a DV defect, the four dangling bonds form two weak covalent bonds of length 2.01 Å, which separate one octagon from two pentagons. A SW defect can be created by a rotation of a carbon-carbon bond at 90 degrees, which transforms the four adjacent hexagons into two pentagons and two heptagons. The relaxation of a nanotube with a SW defect does not yield a strong deformation of the nanotube surface. The relaxed bond between the two pentagons has a length of 1.37 Å. In the cases of a DV and SW defects, there are two other defective nanotube structures but the obtained results for them, as well as for larger supercells and other nanotube types, will be reported elsewhere.

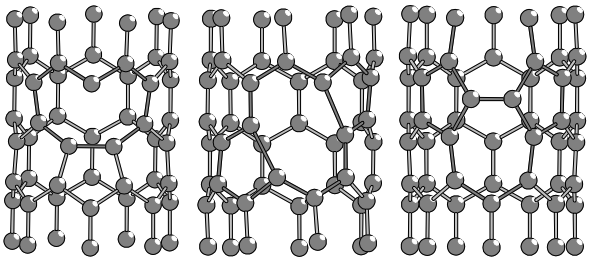

Figure 1 Left, middle, and right: front view of a supercell with a single MV, DV, and SW defect, respectively.

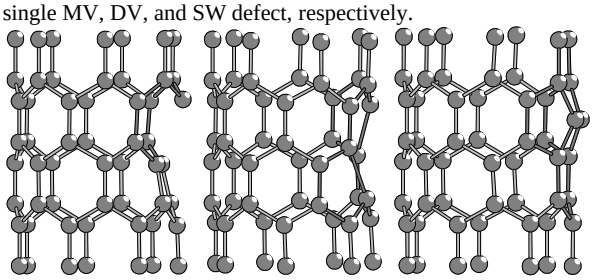

Figure 2 Left, middle, and right: side view of a supercell with a single MV, DV, and SW defect, respectively.

The band structure of nanotube (7,0) changes when defects are created. In particular, the electronic density of states and the optical transition energies, which determine the position and height of the REP of the Raman-active phonons, are also modified. For example, the theoretical second optical transition of perfect tube (7,0) is at 2.93 eV, while for the MV and DV structures it shifts down to about 2.85 eV and for the SW structure three optical transitions appear at 2.72, 2.96, and 3.05 eV.

For perfect nanotube (7,0), there are only two Raman-active phonons, which give rise to intense Raman lines, - the radial-breathing mode (RBM) and the tangential mode (G mode). The REP for these phonons, calculated with electronic excited state width of 0.03 eV, are shown in Fig. 3. For nanotube with defects, due to the lower symmetry of the system more phonons become Raman-active. Moreover, new, defect-associated phonons appear. Figs. 4 – 6 show the four most intense REP of phonons of the three defective structures. Two of these phonons are the RBM and the G-mode, one is a low-frequency deformation mode (DM), and another one is a high-frequency defect-associated mode (DF). Each one of the REP is characterized by two peaks - one at the energy of the incoming resonance and the other at the energy of the out-going resonance. The separation of the two peaks is equal to the phonon energy. In the case of the RBM and the DM, the two peaks overlap considerably because of the small energy of these phonons. It is clearly seen from Figs. 3 – 6 that the REP of the G mode is most intense for the perfect nanotube and it is by 15, 6, and 4 times less intense for nanotubes with a MV, DV, and SW defect, respectively. Thus, the calculations predict a significant decrease of the resonant intensity of the G line in the defective structures.

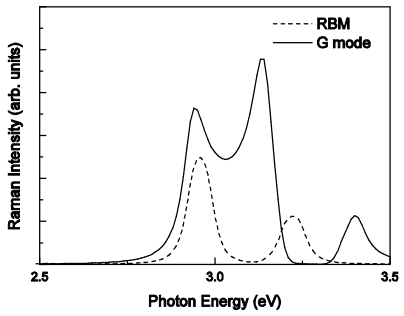

Figure 3 REP of the RBM and the G mode of perfect nanotube (7,0).

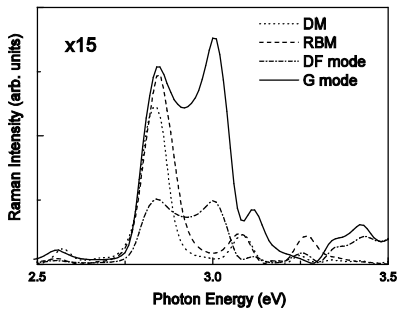

Figure 4 Four most intense REP of phonons of nanotube (7,0) with a single MV defect. The scaling factor is relative to Fig. 3.

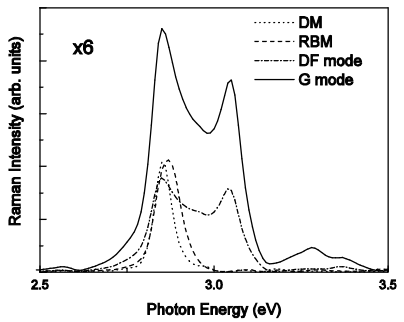

Figure 5 Same as for Fig. 4 but for a single DV defect.

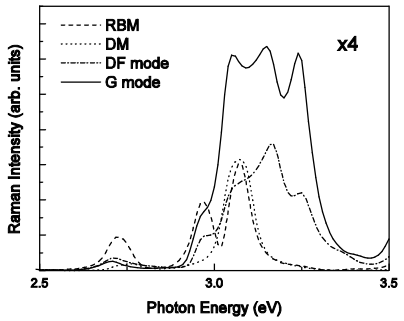

Figure 6 Same as for Fig. 4 but for a single SW defect.

The simulated Raman spectra of the perfect tube and the three defective structures for laser photon energies close to energies of specific optical transitions are shown in Figs. 7 – 10. For the perfect nanotube and for nanotube with a MV (or DV) defect, the photon energy was taken equal to the energy of the second optical transition of 2.93 eV and 2.85 eV, respectively. For nanotube with a SW defect, the second optical transition of the perfect nanotube is split into several transitions. For the simulations of the Raman intensity, we chose the optical transition at 3.05 eV, because it yields high intensity spectra. The phonon linewidth was taken to be 6 cm^{-1}. The smaller scaling factors for Figs. 8 – 10 compared to those for Figs. 4 – 6 result from the enhancement of the Raman intensity for the former because of interference effects of contributions of phonons in the vicinity of the G mode.

Figs. 7 – 10 show that the position of the RBM line remains unchanged upon creating defects. This can be explained by the fact that the RBM is a uniform radial displacement of the atoms of the nanotube and, therefore, depends slightly on the atomic structure and on small departures of the nanotube surface from the ideal cylinder. The intensity of this phonon depends however on the particular atomic structure through the electronic structure and the matrix elements, entering the expression of the intensity.

On the other hand, the line of the G mode is predicted to be observed in a wide region: it should be measured at 1544 cm^{-1} for the perfect nanotube and at 1511 cm^{-1}, 1604 cm^{-1}, and 1567 cm^{-1} for nanotubes with a MV, DV, and SW defect, respectively. The reason for this could be that this phonon depends on the local arrangement of the atoms in the nanotube. There is also at least one DF line in the vicinity of the G mode for each defect structure. They are positioned at 1519 cm^{-1}, 1573 cm^{-1}, and 1612 cm^{-1} for nanotubes with a MV, DV, and SW defect, respectively. Among these three lines, the one at 1519 cm^{-1} for the MV structure should hardly be observed because it overlaps with the G line. The DF lines for the DV and SW structures are well-separated from the G line and should be observed clearly. The DF phonons are localized modes with displacement of atoms close to the particular defect. The atomic displacement pattern of these phonons is quite complicated with the exception of the SW structure. In the latter case, the DF line is predicted at 1612 cm^{-1} and the DF phonon is an almost pure bond-stretching motion of the two atoms, connecting the two pentagons. Previously, the DF line of the metallic nanotube (3,3) with a SW defect has been calculated at 1962 cm^{-1} within the density functional theory [6]. The large difference between the frequencies of this phonon in the two calculations may be due to the difference of the diameters of the two tubes (5.5 Å for nanotube (7,0) and 4.0 Å for nanotube (3,3)), their different band structure (one is semiconducting and the other is metallic), chirality dependence of the DF phonon frequency, and, eventually, the different computational models.

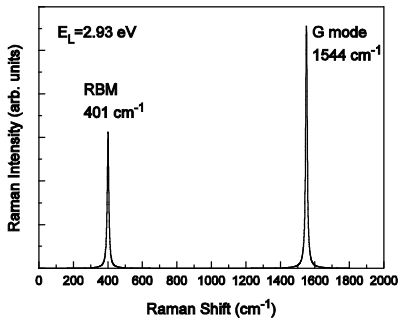

Figure 7 Simulated Raman spectra of perfect nanotube (7,0) for laser excitation energy E_L.

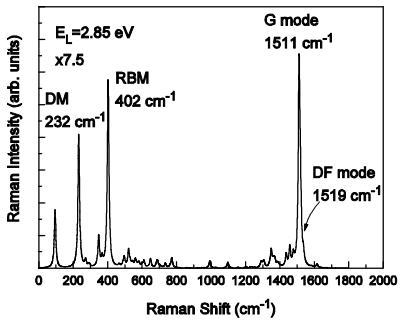

Figure 8 Simulated Raman spectra of nanotube (7,0) with a single MV defect. The scaling factor is relative to Fig. 7.

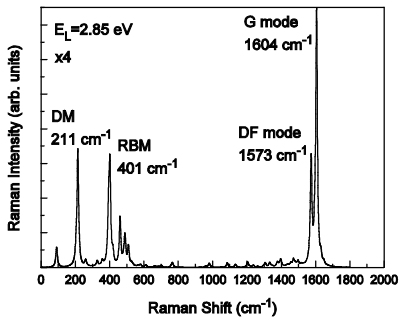

Figure 9 Same as for Fig. 8 but for a single DV defect.

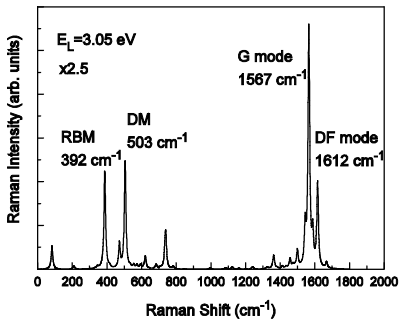

Figure 10 Same as for Fig. 8 but for a single SW defect.

In conclusion, we calculated the resonance Raman spectra of the nanotube (7,0) with a single defect of type monovacancy, divacancy, and Stone-Wales. We identified the phonons, giving rise to high intensity lines, discussed the behaviour of their frequency in the different defective structures and the character of their displacement pattern. These Raman lines can be used as spectroscopic signature of the specific defect.

Acknowledgements V.N.P. was supported partly by the Marie-Curie European Re-integration Grant MERG-CT-2007-201227 within the 7th European Community Framework Programme. V.N.P and Ph.L. acknowledge the support by the NATO Collaborative Linkage Grant CBP.EAP.CLG.982722.

References

[1] M. S. Dresselhaus, G. Dresselhaus, and Ph. Avouris (eds.), Carbon nanotubes: Synthesis, Structure, Properties, and Applications (Springer-Verlag, Berlin, 2001) p. 447.
[2] M. B. Nardelli, J.-L. Fattebert, D. Prlikowski, C. Roland, Q. Zhao, and J. Bernholc, Carbon **38**, 1703 (2000).
[3] P. G. Collins, A. Zettle, H. Bando, A. Thess, and R. E. Smalley, Science **278**, 100 (1997).
[4] J. A. Robertson, E. S. Snow, S. C. Badescu, T. L. Reinecke, and R. F. Perkins, Nano Letters **6**, 1747 (2006).
[5] C. Thomsen, S. Reich, and J. Maultzsch, Phil. Trans. R. Soc. Lond. **362**, 2337 (2004).
[6] Y. Miyamoto, A. Rubio, S. Berber, M. Yoon, and D. Tománek, Phys. Rev. B **69**, 121413(R) (2004).
[7] G. Wu and J. Dong, Phys. Rev. B **73**, 245414 (2006).
[8] H. Y. He and B. C. Pan, Phys. Rev. B **77**, 073410 (2008).
[9] S. Malola, H. Häkkinen, and P. Koskinen, Phys. Rev. B **77**, 155412 (2008).
[10] V. N. Popov and L. Henrard, Phys Rev B **70**, 115407 (2004).
[11] V. N. Popov and Ph. Lambin, Phys Rev B **73**, 085407 (2006).
[12] V. N. Popov, L. Henrard, and Ph. Lambin, Phys Rev B **72**, 035436 (2005).